PERGAMON

International Journal of Heat and Mass Transfer 43 (2000) 2047–2052

International Journal of HEAT and MASS TRANSFER

www.elsevier.com/locate/ijhmt

Technical Note

A model of microsegregation during binary alloy solidification

V.R. Voller*

Saint Anthony Falls Laboratory, Civil Engineering, University of Minnesota, Mississippi River at 3rd Avenue SE, Minneapolis, MN 55414, USA

Received 10 December 1998; received in revised form 18 August 1999

1. Introduction

A comprehensive model of alloy solidification requires the coupling of macro scale heat and mass transport with local scale phenomena occurring in the solid–liquid microstructure. A key local scale phenomenon is microsegregation — the partitioning and redistribution of the solutes at the solid–liquid interface. In most systems, the solutes are well mixed in the liquid phase and microsegregation is controlled by solute diffusion in the solid phase; a process referred to as "back-diffusion".

Microsegregation models are of two types, complete numerical models [1–3], or semi-analytical and approximate relationships [4–8]. Recent work by the author has focused on developing a range of approximate microsegregation relationships [9–12]. The completion of this work however, required the building of a complete numerical model for benchmarking of the approximate relationships. The aim of this note is to provide a detailed report of this numerical model, which has not previously been presented in the literature. The proposed model is similar in concept to the recent work of Yoo and Kim [8] where the back-diffusion, under the condition of a prescribed cooling rate, is modeled with a parabolic profile assumption. In contrast, in this work a full numerical treatment of back-diffusion is invoked and both a prescribed cooling rate and parabolic solid growth model are developed.

2. The microsegregation model

A dilute binary eutectic alloy (e.g., aluminum–copper) will be used as an example material. This alloy solidifies over a temperature range that defines a solid–liquid mushy region, which is assumed to have a dendritic microstructure (see Fig. 1). The characteristic length scale for microsegregation is the secondary arm spacing, which will increase in length (coarsen) [13,14], as the solidification proceeds. As such, the domain of the microsegregation model will be a representative half-secondary arm space, $X_0(t)$. Appropriate assumptions in this domain are: (1) mass diffusion in the liquid is complete, i.e., at any point in time, the solute concentration in the liquid phase C_1 is uniform; (2) equilibrium is maintained at the solid–liquid interface, i.e., $C_s^i = kC_1$; (3) the liquidus line is straight; and (4) at any point in time, due to the relatively rapid rate of heat diffusion, the temperature in the arm spacing is uniform.

The central component in the microsegregation model is the solute balance in the half-arm spacing, which can be written as

$$\int_0^{X_s} C_s \, dx + (X_0 - X_s)C_1 = X_0 C_0 \tag{1}$$

where X_s is the length of the solid phase in the half-

* Tel.: +1-612-625-0764; fax: +1-612-626-7750.
E-mail address: volle001@tc.umn.edu (V.R. Voller).

0017-9310/00/$ - see front matter
PII: S0017-9310(99)00268-9

arm space. Progress is made on introducing dimensionless space and time variables

$$\eta = \frac{x}{X_{\text{final}}}, \quad \tau = \frac{t}{t_{\text{final}}} \tag{2}$$

where the superscript "final" indicates the value at the final solidification point. In terms of the new space variable the solute balance can be written as

$$\int_0^{\eta_s} C_s \, d\eta + (\eta_0 - \eta_s) C_1 = \eta_0 C_0. \tag{3}$$

On differentiating with respect to τ

$$\int_0^{\eta_s} \frac{\partial C_s}{\partial \tau} \, d\eta + (k-1) C_1 \frac{d\eta_s}{d\tau} + (\eta_0 - \eta_s) \frac{dC_1}{d\tau} + (C_1 - C_0) \frac{d\eta_0}{d\tau} = 0. \tag{4}$$

where it has been assumed that the average composition in the arm space remains fixed at the initial value of C_0, i.e., no macrosegregation. Further simplification is made on noting that in the solid part of the domain, $0 \le \eta \le \eta_s$, the solute diffusion is governed by

$$\frac{\partial C_s}{\partial \tau} = \alpha \frac{\partial^2 C_s}{\partial \eta^2} \tag{5}$$

where

$$\alpha = \frac{D t_{\text{final}}}{X^2_{\text{final}}} \tag{6}$$

is a Fourier number and D is the mass diffusivity in the solid. Substitution of Eq. (5) in Eq. (4) gives, after expanding the integral,

$$\alpha \frac{\partial C_s}{\partial \eta}\bigg|_{\eta=\eta_s} + (k-1) C_1 \frac{d\eta_s}{d\tau} + (\eta_0 - \eta_s) \frac{dC_1}{d\tau} + (C_1 - C_0) \frac{d\eta_0}{d\tau} = 0. \tag{7}$$

This is the governing equation for the solute balance. The first term is the back-diffusion of solute into the solid phase, the next two terms account for the redistribution of solute due to the movement of the solid–liquid front, and the last term accounts for solute entering the domain due to coarsening.

Equation (7) is solved with a time marching numerical solution with the initial conditions $\eta_s = 0$, $C_1 = C_0$, and $\partial C_s/\partial \eta|_{\eta=0} = 0$. In this solution, the back-diffusion term is calculated using a deforming finite difference

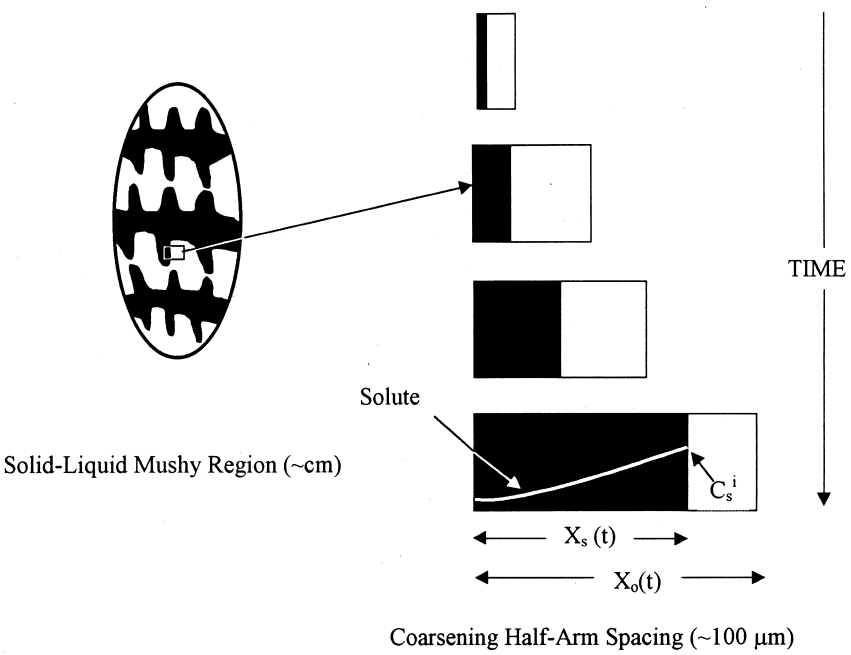

Fig. 1. Solidification and coarsening in a solidifying half-dendrite arm space.

method (see detailed discussion below) and the coarsening is modeled as

$$\eta_0 = \tau^n, \quad \frac{d\eta_0}{d\tau} = n\tau^{n-1} \tag{8}$$

where n ($\sim(1/3)$ [13]) is a coarsening exponent.

To complete the solution of Eq. (7) it is necessary to prescribe the rate of change of the liquid concentration or the solid fraction in the arm spacing. This choice leads to two alternative versions of the microsegregation model.

2.1. A constant rate model

In this version of the model, the arm space cools at a prescribed constant rate and it follows, from the assumptions of a uniform liquid concentration and a straight liquidus, that

$$\frac{dC_1}{d\tau} = (C_0 - C_{end}). \tag{9}$$

Solidification terminates at the prescribed composition $C_1 = C_{end}$, and Eq. (7) is solved for the growth of the solid. An Euler treatment gives the following time marching solution

$$\eta_s = \eta_s^{old} + \Delta\tau\left[\frac{BD^{old} + (\eta_0 - \eta_s^{old})(C_0 - C_{eut}) + (C_1 - C_0)n\tau^{n-1}}{(1-k)C_1}\right] \tag{10}$$

where $\Delta\tau$ is the simulation time step, BD is an approximation for the back-diffusion term and the superscript "old" indicates evaluation at the old time step. Where possible, values in the function on the RHS of Eq. (10) are evaluated at the current time step. The exceptions are the back-diffusion term, BD, and the solid length η_s. Strictly, within each time step, an iterative solution should be used that updates these values. In practice, however, it is found that using a small time step with a single iteration of Eq. (10) is effective.

2.2. A parabolic growth model

In this version of the model the growth of the solid fraction ($f_s = \eta_s/\eta_0$) in the half-arm space is parabolic in time. In terms of the solid length

$$\eta_s = \eta_0\tau^{1/2}, \quad \frac{d\eta_s}{d\tau} = n\tau^{n-1} + \frac{1}{2}\eta_0\tau^{-1/2}. \tag{11}$$

Solidification terminates at the prescribed solid length $\eta_s = \eta_{end}$ and Eq. (7) is solved for the liquid solute concentration. An Euler solution gives the following time marching solution

$$C_1 = C_1^{old} + \Delta\tau\left[\frac{BD^{old} + (k-1)C_1^{old}\frac{d\eta_s}{dt} + (C_1^{old} - C_0)n\tau^{n-1}}{\eta_s - \eta_0}\right]. \tag{12}$$

Values on the RHS of Eq. (12) should be evaluated at the current time and in the strict sense, iteration in the time step is required to update the back-diffusion term, BD, and the liquid concentration C_1. As with the constant rate model, however, a small time step and a single application of Eq. (12) is sufficient.

Estimation of the back-diffusion term, BD, in the Euler solution (Eq. (10) or Eq. (12)) requires the calculation of the solute profile, controlled by diffusion, in the solid domain of the half-arm spacing. This domain, $0 \le \eta \le \eta_s(\tau)$, is deforming in time and it is convenient to carry out any analysis in the transformed domain defined by the Landau transformation [15] $\xi = \eta/\eta_s(t)$. In this transformation, the solid domain, $0 \le \xi \le 1$, remains fixed in time and the diffusion equation for the solid solute (dropping the subscript "s" for notation convenience) is

$$\frac{\partial C}{\partial \tau} = \alpha\frac{\partial^2 C}{\partial \eta^2} + \left[\frac{\eta}{\eta_s}\frac{d\eta_s}{d\tau}\right]\frac{\partial C}{\partial \eta} \tag{13}$$

subject to the boundary conditions

$$\left.\frac{\partial C}{\partial \eta}\right|_{\eta=0} = 0, \quad \text{and} \quad C|_{\eta=\eta_s} = kC_1(\tau) \tag{14}$$

and the initial condition

$$C = C_0. \tag{15}$$

Note the time derivative on the LHS of Eq. (13) is evaluated at constant values of the transformed variable ξ and the bracketed term on the RHS is the velocity of a constant ξ point in real space η. A rearrangement of Eq. (13) is

$$\frac{1}{\eta_s}\frac{\partial(\eta_s C)}{\partial \tau} = \alpha\frac{\partial^2 C}{\partial \eta^2} + \frac{\partial}{\partial x}\left(C\frac{\eta}{\eta_s}\frac{d\eta_s}{dt}\right). \tag{16}$$

A discretization of this equation, on a uniform grid of m nodes that deforms with the solid growth, leads to the following time implicit finite difference scheme at node point P

$$\frac{C_P\Delta\eta - C_P^{old}\Delta\eta^{old}}{\Delta\tau\Delta\eta} = \alpha\frac{C_E - 2C_P + C_W}{\Delta\eta^2} + \frac{V_{east}C_E - V_{west}C_P}{\Delta\eta}. \tag{17}$$

The following points concerning Eq. (17) are noted.

Table 1
Basic comparisons of the Constant Rate Model with limiting analytical solutions for the solid fraction, f ($k = 0.16$, $C_0 = 4.9$, and $C_{end} = 20$)

Analytical equation	Analytical value of f	Model prediction of f
Eq. (20)	0.81258	0.81260
Eq. (21)	0.89881	0.89871
Eq. (22)	0.82760	0.82790

1. The subscripts "W" and "E" are for nodal values to the east and west of point P, the subscript "west" and "east" refer to values at the mid points between nodes, the term $\Delta\eta$ is the grid spacing, the superscript "old" refers to old time values, and

$$V_{west} = \frac{\eta_{west}}{\eta_s}\frac{d\eta_s}{dt} \quad \text{and} \quad V_{east} = \frac{\eta_{east}}{\eta_s}\frac{d\eta_s}{dt}$$

   are the velocities of the control volume interfaces.
2. In the constant rate model the solid growth is approximated as $d\eta_s/dt = (\eta_s - \eta_s^{old})/\Delta\tau$, with the value of η_s taken from LHS of Eq. (10). In the parabolic growth model $d\eta_s/dt$ is evaluated directly by Eq. (11).
3. Upwinding has been used to treat the grid advection terms.
4. At the boundary $\eta = 0$ (node 1) Eq. (17) becomes

$$\frac{C_P\Delta\eta - C_P^{old}\Delta\eta_P^{old}}{2\Delta\tau\Delta\eta} = \alpha\frac{C_E - C_P}{\Delta\eta^2} + \frac{V_{east}C_E}{\Delta\eta} \tag{18}$$

5. The finite difference equations are closed on noting that at the solid–liquid interface $C_m = kC_1$.

At each time step solution of the finite difference equations — a tri-diagonal matrix algorithm can be used—will provide the solute distribution in the solid. From this distribution the back-diffusion term can be approximated using a second order difference, i.e.,

$$BD = \left.\frac{\partial C}{\partial\eta}\right|_{\eta_s} = \alpha\frac{3C_m - 4C_{m-1} + C_{m-2}}{2\Delta\eta}. \tag{19}$$

3. Validation

There are four limiting analytical solutions that can be use as basic test cases for the proposed microsegregation model.

1. In the limit of complete diffusion in the solid $\alpha \to \infty$ the microsegregation in the arm spacing is describe by the lever rule [16],

$$f = \frac{\eta_s}{\eta_0} = \frac{1}{1-k}\left(1 - \frac{C_0}{C_1}\right) \tag{20}$$

   which is independent of the solidification path or the nature of the coarsening.
2. In the limit of zero solute diffusion in the solid $\alpha = 0$ and no coarsening, microsegregation is described by the Gulliver–Scheil equation [17]

$$f = \frac{\eta_s}{\eta_0} = 1 - \left[\frac{C_1}{C_0}\right]^{1/(k-1)}. \tag{21}$$

   This relationship is independent of the solidification path, i.e., the expression is valid for both the constant rate and parabolic growth.
3. In the limit of zero solute diffusion in the solid $\alpha = 0$ and coarsening governed by Eq. (8), Mortensen [14] has derived the following analytical microsegregation relationship for an arm space cooled at a constant rate

$$f = \frac{\eta_s}{\eta_0} = \frac{1+n}{1-k}\frac{C_1^{[1/(k-1)]}}{(C_1 - C_0)^n}\int_{C_0}^{C_1}\phi^{[k/(1-k)]}(\phi - C_0)^n\,d\phi. \tag{22}$$

4. In the limit of zero solute diffusion in the solid $\alpha = 0$ and coarsening governed by Eq. (8), Voller and Beckermann [11] have derived the following analytical microsegregation relationship for an arm space with a parabolic growth rate of the solid fraction

Table 2
Basic comparisons of the parabolic growth rate model with limiting analytical solutions ($k = 0.16$, $C_0 = 4.9$, and $f_{end} = 0.75$)

Analytical equation	Analytical value of kC_1/C_0	Model prediction of kC_1/C_0
Eq. (20)	0.51181	0.50736
Eq. (21)	0.43200	0.43103
Eq. (23)	0.49680	0.49720

Table 3
Values of the ratio kC_1/C_0 on complete solidification [comparison of Kobayashi [18] analytical solution with predictions obtained using the parabolic growth rate model)

	$\alpha = 0.05$		$\alpha = 0.15$		$\alpha = 0.5$	
	Analytical	Model	Analytical	Model	Analytical	Model
$k = 0.2$	13.60	13.39	5.92	5.94	2.60	2.50
$k = 0.4$	4.78	4.83	2.65	2.66	1.56	1.56

$$\frac{C_1}{C_0} = \frac{2n(1-f)^{(1+2n)k-1}}{f^{2n}} \int_0^f \phi^{2n-1}(1-\phi)^{-(1+2n)k}\,\mathrm{d}\phi. \tag{23}$$

In Table 1, using aluminum–copper alloy data, the performance of the proposed constant rate microsegregation model is compared against the limiting solutions, Eqs. (20–22). The parabolic growth model is compared against the limiting analytical solutions, Eqs. (20), (21) and (23), in Table 2. In both comparisons the agreement between the model and analytical results is excellent. In all cases reported, converged model solutions are obtained with 2000 time steps. In matching the lever rule predictions 500 space steps are used in the back-diffusion treatment and the Fourier number is set to the high value of $\alpha = 20$. Where appropriate, the coarsening coefficient is set at $n = 1/3$ [13].

In the case of parabolic growth and no coarsening Kobayashi [18] has developed and presented an analytical solution for microsegregation which includes back-diffusion. For a range of Fourier numbers and partition coefficients, Kobayashi reports analytical values of the maximum segregation ratio — i.e., the ratio kC_1/C_0 — at the point where the solid fraction $f = 1$ (complete solidification). Predictions of the maximum segregation ratio, obtained with the parabolic growth model, are compared with the analytical solutions in Table 3. The comparison is reasonably good with the maximum relative error not exceeding 2%.

With reference to the results in Table 3 it is noted that: (1) the parabolic growth model will only work if the prescribed end value of the solid fraction is $f_{\mathrm{end}} < 1$; and (2) as the solid fraction approaches unity there is a very rapid increase in the solute concentration in the liquid. Hence, predicting values close to the analytical maximum segregation level is a numerical challenge. The model results reported in Table 3 are obtained by linearly extrapolating parabolic growth model predictions from two high values of f_{end}. In most cases the values $f_{\mathrm{end}} = 0.999$ and $f_{\mathrm{end}} = 0.9995$ are used, at large values of k and α, however, due to poor convergence, it is necessary to reduce the values to $f_{\mathrm{end}} = 0.99$ and $f_{\mathrm{end}} = 0.995$.

In all applications of the parabolic growth model 8000 time steps in the Euler solution and 500 space steps in the back-diffusion solution are used. These values were reached after a convergence study.

In a binary-eutectic alloy when the liquid concentration reaches the eutectic, $C_1 = C_{\mathrm{eut}}$, a non-equilibrium second phase is precipitated and the remaining liquid forms a solid eutectic of fixed average composition. Using a Bridgeman furnace Sarreal and Abbaschian [19] conducted experiments to determine the effect of solidification time, t_{final}, on the fraction of eutectic that forms in an aluminum–4.9% copper alloy. Table 4 gives the measured eutectic fractions against Fourier number. Note that: (1) the reported eutectic values in Table 4 are obtained by converting the nonequlibrium second phase values reported by Sarreal and Abbaschain, see Voller and Sundarraj [3] for details; (2) the final arm spacing are obtained using a Kirkwood [13] coarsening model of the form $\lambda = 2X_0 = 9.4t_f^{1/3}$ [10], which has a coarsening exponent of $n = 1/3$; (3) the eutectic concentrtaion is $C_{\mathrm{eut}} = 33.2\%$; and (4) a constant diffusion value of $D = 5 \times 10^{-13}$ m^2/s is used.

Fig. 2 compares the predictions of the constant rate model with the measured values. In the constant rate model $C_{\mathrm{end}} = C_{\mathrm{eut}}$, when this point is reached the frac-

Table 4
Measured values of eutectic fraction

Solidification time t_f (s)	0.52	1.51	8.72	93.3	980
Arm spacing $\lambda = 2X_0$ (μm)	7.56	10.78	19.35	42.63	93.35
Fourier No. $\alpha = Dt_f/X_o^2$	0.0182	0.0260	0.0466	0.1027	0.2249
% Fraction of eutectic	7.5	7.16	6.84	6.52	5.54

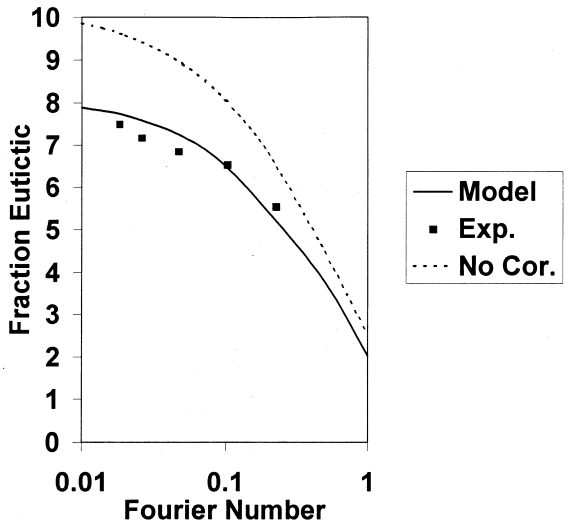

Fig. 2. Comparison of the constant rate model with experimental measurements.

tion of eutectic is given by $(1-\eta_s)$. Agreement between the model and experimental predictions is good. As a point of comparison the eutectic predictions obtained with no coarsening ($n = 0$) are also shown, this provides a graphical reference for the effect of coarsening on the microsegregation.

4. Conclusions

Modeling microsegregation is a key component in a comprehensive solidification model. Usually, due to resource limitations, only approximate microsegregation relationships are used in large-scale solidification analysis. For this approach to be valid, however, it is important that the performance of the approximation is checked against complete and detailed numerical microsegregation models. This paper has presented two versions of a numerical microsegragtion models that can be used for this purpose. In the first version of the model, the solidification is controlled by a constant cooling rate. In the second, a parabolic growth rate is assumed. Both models account for back-diffusion of solute into the solid and coarsening of the arm space.

The models are checked and validated by comparing with limiting analytical solutions and experimental measurements. These comparisons indicate that both versions of the model function correctly and can provide accurate and practical predictions.

Copies of documented Fortran codes for the two versions of the microsegregation models can befound at the following web site http://www.ce.umn.edu/ ~ voller.

References

[1] A. Roósz, E. Halder, H.E. Exner, Numerical calculation of microsegregation in coarsened dendritic microstructures, Mater. Sci. Technol. 2 (1986) 1149–1155.
[2] T.P. Battle, R.D. Pehlke, Mathematical modeling of microsegregation in binary metallic alloys, Metallurgical Transactions 21B (1990) 357–375.
[3] V.R. Voller, S. Sundarraj, Modelling of microsegregation, Mater. Sci. Technol. 9 (1993) 474–481.
[4] H.D. Brody, M.C. Flemings, Solute redistribution during dendritic solidification, Trans. Met. Soc. AIME 236 (1966) 615–624.
[5] T.W. Clyne, W. Kurz, Solute redistribution during solidification with rapid solid state diffusion, Metallurgical Transactions 12A (1981) 965–971.
[6] I. Ohnaka, Mathematical analysis of solute redistribution during solidification with diffusion in solid phase, Transactions ISIJ 26 (1986) 1045–1051.
[7] C.Y. Wang, C. Beckermann, Unified solute diffusion model for columnar and equiaxed dendritic alloy solidification, Material Science and Engineering 171 (1993) 199–211.
[8] H. Yoo, C.-J. Kim, A refined solute diffusion model for columnar dendritic alloy solidification, Int. J. Heat Mass Transfer 41 (1998) 4379–4383.
[9] V.R. Voller, A semi-analytical model of microsegregation in a binary alloy, Journal of Crystal Growth 197 (1999) 325–332.
[10] V.R. Voller, A semi-analytical model of microsegregation and coarsening in a binary alloy, Journal of Crystal Growth 197 (1999) 333–340.
[11] V.R. Voller, C. Beckermann, A unified model of microsegregation and coarsening, Metallurgical Transactions A, in press (1999).
[12] V.R. Voller, C. Beckermann, Approximate models of microsegregation with coarsening, Metallurgical Transactions A (1999) (in press).
[13] D.H. Kirkwood, A simple model for dendrite arm coarsening during solidification, Material Science and Engineering 73 (1985) L1–L4.
[14] A. Mortensen, On the influence of coarsening on microsegregation, Metallurgical Transactions 20A (1989) 247–253.
[15] J. Crank, Free and Moving Boundary Problems, Clarendon Press, Oxford, 1984.
[16] M. Flemings, Solidification Processing, McGraw-Hill, New York, 1984.
[17] G.M. Gulliver, Metallic Alloys, Griffen, London, 1922.
[18] S. Kobayashi, Solute redistribution during solidification with diffusion in solid phase: a theoretical analysis, Journal of Crystal Growth 88 (1988) 87–96.
[19] J.A. Sarreal, G.J. Abbaschian, Effect of solidification rate on microsegregation, Metallurgical Transactions 17A (1986) 2063–2073.